Available online at www.sciencedirect.com
ScienceDirect
Trans. Nonferrous Met. Soc. China 30(2020) 2613−2624
Transactions of Nonferrous Metals Society of China
www.tnmsc.cn

Severe plastic deformation of commercially pure aluminum using novel equal channel angular expansion extrusion with spherical cavity

Xiao-xi WANG[1], Xiang ZHANG[2,3], Xin-yu JING[1], Jun-chi YUAN[1] , Wei SONG[1]

1. School of Mechanical and Electrical Engineering, Xuzhou University of Technology, Xuzhou 221018, China;
2. Jiangsu XCMG Construction Machinery Research Institute Co., Ltd., Xuzhou 221004, China;
3. State Key Laboratory of Intelligent Manufacturing of Advanced Construction Machinery, Xuzhou Construction Machinery Group, Xuzhou 221004, China

Received 15 February 2020; accepted 4 May 2020

Abstract: Equal channel angular expansion extrusion with spherical cavity (ECAEE-SC) was introduced as a novel severe plastic deformation (SPD) technique, which is capable of imposing large plastic strain and intrinsic back-pressure on the processed billet. The plastic deformation behaviors of commercially pure aluminum during ECAEE-SC process were investigated using finite element analysis DEFORM-3D simulation software. The material flow, the load history, the distribution of effective strain and mean stress in the billet were analyzed in comparison with conventional equal channel angular extrusion (ECAE) process. In addition, single-pass ECAEE-SC was experimentally conducted on commercially pure aluminum at room temperature for validation, and the evolution of microstructure and microhardness of as-processed material was discussed. It was shown that during the process, the material is in the ideal hydrostatic stress state and the load requirement for ECAEE-SC is much more than that for ECAE. After a single-pass ECAEE-SC, an average strain of 3.51 was accumulated in the billet with homogeneous distribution. Moreover, the microstructure was significantly refined and composed of equiaxed ultrafine grains with sub-micron size. Considerable improvement in the average microhardness of aluminum was also found, which was homogenized and increased from HV 36.61 to HV 70.20, denoting 91.75% improvement compared with that of the as-cast billet.

Key words: severe plastic deformation; equal channel angular expansion extrusion with spherical cavity (ECAEE-SC); numerical simulation; strain accumulation; grain refinement

1 Introduction

With the rapid development of material science and technology, higher performance requirements have been proposed for the advanced materials. Grain refinement is an effective way to improve the comprehensive properties of the materials [1]. In the last decades, severe plastic deformation (SPD) method, which aims at microstructure controlling, has been widely concerned and investigated due to its excellent grain refinement ability and the great role in the improvement of strength and toughness for the materials [2−4]. Among these methods, equal channel angular extrusion (ECAE) is known as one of the most representative and promising techniques for fabricating ultrafine grained (UFG) materials [5,6]. The unique property of ECAE process is the possibility of accumulating extremely

Foundation item: Project (51905462) supported by the National Natural Science Foundation of China; Project (BK20200297) supported by the Natural Science Foundation of Jiangsu Province, China; Project (GDZB-127) supported by Jiangsu Provincial "Six Talent Peaks" Program, China; Project (2018202) supported by the "Youth Science and Technology Talents" Sponsored Program of Jiangsu Science and Technology Association, China
Corresponding author: Xiao-xi WANG; Tel: +86-516-83105376; E-mail: wxx19851109@sina.com
DOI: 10.1016/S1003-6326(20)65406-1

large plastic strains through repeated extrusions and route alterations without changing the initial cross-sections of the billet. However, it is generally necessary to perform a large number of passes to obtain well-defined and stable microstructure [7]. As the processing of ECAE is discontinuous essentially, the billet should be removed from the die when conducting multiple passes of extrusion, which significantly reduces the process efficiency and thus limits its industrial applications [8,9]. Therefore, it is of great importance to develop new SPD techniques to tackle the problems of discontinuous deformation and low process efficiency.

Recently, the combination of ECAE and other SPD methods or conventional processes (e.g. extrusion and rolling) has been gradually explored to increase the process efficiency by inducing larger imposed strain during an individual pass to reduce the number of passes [10]. Several novel SPD processes are now available and intensive investigations have been conducted. These include equal channel angular pressing and torsion (ECAPT) [11], spiral equal channel angular extrusion (Sp-ECAE) [12], non-equal channel lateral extrusion (NECLE) [13], incremental equal channel angular pressing (I-ECAP) [14], half channel angular extrusion (HCAE) [15] and expansion equal channel angular extrusion (Exp-ECAE) [16], etc.

In the present study, a novel technique named equal channel angular expansion extrusion with spherical cavity (ECAEE-SC) was proposed based on the conventional ECAE process. In this modification, the combination of upsetting, shear, expansion and extrusion was performed simultaneously on the processed billet in an individual pass, thus imposing higher values of plastic strain as well as providing an ideal hydrostatic stress state for as-processed material. Commercially pure aluminum was subjected to single-pass of ECAEE-SC. Plastic deformation behaviors in terms of the material flow, the load history, the distribution of effective strain and mean stress were analyzed via three dimensional numerical simulations based on the finite element method (FEM). In addition, the subsequent experiment was conducted on the self-designed ECAEE-SC die at room temperature to obtain grain refinement and microhardness improvement, which represented a verification of the predicted simulation results as well.

2 Principle of ECAEE-SC process

The schematic diagram of ECAEE-SC process is illustrated in Fig. 1. As shown in Fig. 1(a), ECAEE-SC die is modified based on the conventional ECAE process by arranging a spherical cavity at the intersection of channels and a horizontal expansion channel at the exit channel, which could facilitate the metal flow and improve the die filling. In particular, this novel process has a high efficiency for material forming by integrating deformations of upsetting, shear, expansion and extrusion in a single die for each pass. Therefore, larger effective strains could be accumulated, realizing the possibility of “one pass extrusion, different and continuous deformations”.

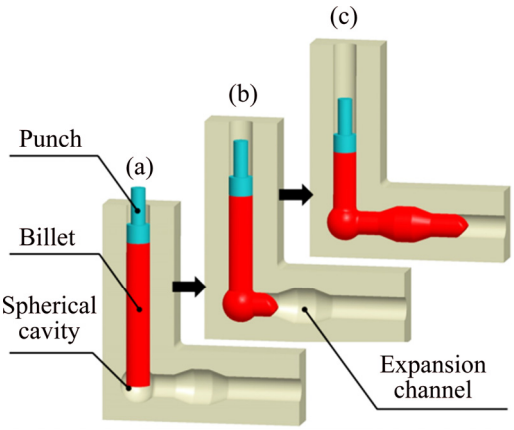

Fig. 1 Schematic diagram of sequence of typical ECAEE-SC prooess: (a) Initial state; (b) At spherical cavity; (c) In expansion channel

In detail, the ECAEE-SC die typically consists of five main deformation zones including entry channel, spherical cavity, transition channel, expansion channel and exit channel, respectively. As the channels of all containers have to be filled with the material during the process, a plug should be placed at the end of exit channel for the first pass extrusion. Once the expansion channel is filled, the plug is removed. The extruded material then acts as a plug and provides an intrinsic back-pressure to ensure a complete die filling in the expansion channel.

During ECAEE-SC process, the billet is first

inserted into the entry channel and upset by a punch. Due to the forward movements of the billet, it is subjected to the intense plastic strain at the spherical cavity, where the pure shear and expansion occur simultaneously (Fig. 1(b)). As the billet leaves the spherical cavity, it recovers initial cross-section. Afterwards, the billet locally expands in the expansion channel (Fig. 1(c)) where the material keeps full during the process. The reduction of the channel diameter and friction in the latter part of expansion channel result in forces acting opposite the extrusion direction, creating a high level of hydrostatic pressure on the processed billet. Once a billet is extruded to the exit channel for the whole length, the process is stopped. The punch is raised and the next billet is loaded into the container, then the second pass starts. Subsequently, the entire billet is deformed and finally leaves the extrusion die by "billet to billet". Since the main dimensions of the billet remain unchanged when it leaves the die, it is possible to repeat the operation as much as required for obtaining larger plastic strains, which helps to attain UFG microstructure and thus achieves excellent mechanical properties.

3 Experimental

3.1 Finite element simulation

Plastic deformation behaviors of ECAEE-SC process were investigated using commercially available FEM package DEFORM-3D V6.1 software. The FEM model of ECAEE-SC is shown in Fig. 2(a). The simulation was conducted on commercially pure aluminum billet with 15 mm in diameter and 100 mm in height. Material characteristics implemented in the simulation were defined according to the flow stress equation available in the software [17] and depicted as $\bar{\sigma}=\sigma(\bar{\varepsilon},\dot{\bar{\varepsilon}},T)$, where $\bar{\sigma}$, $\bar{\varepsilon}$, $\dot{\bar{\varepsilon}}$ and T are the flow stress, the effective strain, the effective strain rate and the temperature, respectively.

The geometrical parameters of ECAEE-SC die channel are shown in Table 1, which are identical to those of experiment and allow for the direct comparison of simulation results with those obtained experimentally. The punch and the bottom die were defined as rigid bodies (H13 tool steel) to ignore very small deformations in the equipment. The initial billet was meshed into 40000 tetrahedral deformable elements with a size ratio of 2 (Fig. 2(b)), which was found to be sufficient relative to the numerical accuracy and computational efficiency by varying the number of elements. Automatic re-meshing was also activated to accommodate large strains during the simulations and direct iteration method solver was implemented. Shear friction model was used in the present work, and the friction coefficient value of 0.12 was assumed to simulate interaction conditions between the billet and the die, which is a recommended value during cold metal forming using a steel die in DEFROM-3D V6.1 [18]. Finally, the simulation was performed at room temperature (20 °C) with a punch speed of 1 mm/s, and the constant displacement of 0.25 mm per step was given as input parameter in the simulation controls.

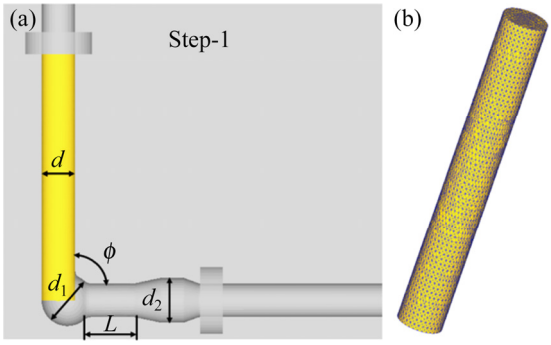

Fig. 2 FEM model of ECAEE-SC process (a) and initial meshing of processed billet (b)

Table 1 Geometrical parameters of ECAEE-SC die channel

Channel diameter, d/mm	Die angle, ϕ/(°)	Diameter of spherical cavity, d_1/mm	Length of transition channel, L/mm	Diameter of expansion channel, d_2/mm
15	90	23	30	20

3.2 Material and method

The as-cast commercially pure aluminum (1060) was used as the initial material in the present study. The chemical composition of the material is indicated in Table 2. Cylindrical billets with a diameter of 15 mm and a height of 80 mm were machined from 1060 aluminum ingot. The extruded billets were annealed at 150 °C for 1 h and then furnace-cooled to room temperature to obtain a homogeneous microstructure.

Table 2 Chemical composition of commercially pure aluminum (wt.%)

Fe	Mn	Mg	Si	Zn	Ti	Cu	Al
<0.35	<0.03	<0.03	<0.25	<0.05	<0.03	<0.05	>99.6

ECAEE-SC process was performed on the YD32G−100 hydraulic press with the extrusion speed of 1 mm/s. The photograph of a self-designed split die is shown in Fig. 3(a). MoS_2 spray was used for lubrication to diminish the friction effect between interface of the die and the processed billet. The billet was extruded from the entry channel to the spherical cavity and then, from the expansion channel to the exit channel, as can be seen in Fig. 3(b). After one pass of extrusion, the complement tests including microstructure characterization and microhardness measurement were performed to investigate the effects of ECAEE-SC process on the microstructure characteristics and mechanical properties of commercially pure aluminum. To verify the effectiveness of ECAEE-SC process, the results were compared with experimental results of one pass ECAE under the same deformation condition.

Samples for microscopic characterization were cut on the cross-section perpendicular to the billet axes. After grinding, mechanical polishing and electrochemical polishing, analyses of grains were performed using a JSM−7001F field emission scanning electron microscope (SEM) with electron backscattered diffraction (EBSD), while the substructure induced by the applied deformation was observed on a JEM−2010 high resolution transmission electron microscope (TEM). TEM foils were prepared using a twin-jet electropolishing device. The electrolyte was 60% CH_3OH + 35% $C_4H_{10}O$ + 5% $HClO_4$ (volume fraction), and the electrolysis temperature was about −30 °C. Vickers microhardness (HV) tests were carried out on a KB30S microhardness tester with a load of 100 g and a dwell time of 15 s. In order to analyze the homogeneity of the mechanical properties over the sample cross-section, the measurements were performed at the selected 15 points uniformly distributed along the diameter with a spacing of 1 mm, and then the average value was reported.

4 Results and discussion

4.1 Material flow during ECAEE-SC process

Figure 4 shows features of the material flow during ECAEE-SC process. It is observed that the finite element meshes are severely sheared along the flow direction due to a very high strain imposed on the billet, as indicated by circles in Fig. 4(a). During ECAEE-SC process, the metal flow is continuous and relatively steady. As the spherical cavity plays the role of “split-flow” and generates a “vortex-like” flow pattern (Fig. 4(b)), the die filling at spherical corner is significantly improved and consequently, the corner gap between the billet and the outer corner of the die is invisible (Fig. 4(c)). Having passing through the transition channel, the billet is continuously extruded into the expansion channel and endured a hydrostatic pressure where the contact area between the billet and die walls increases as a result of the back pressure applied at the exit channel. It is clearly seen in Fig. 4(c) that in the process of ECAEE-SC, the contact area between the billet and the die walls increases, leading to a rather completely filling of the die channel especially in two main deformation zones (the spherical cavity and the expansion channel). In addition, due to the severe shear and high pressure

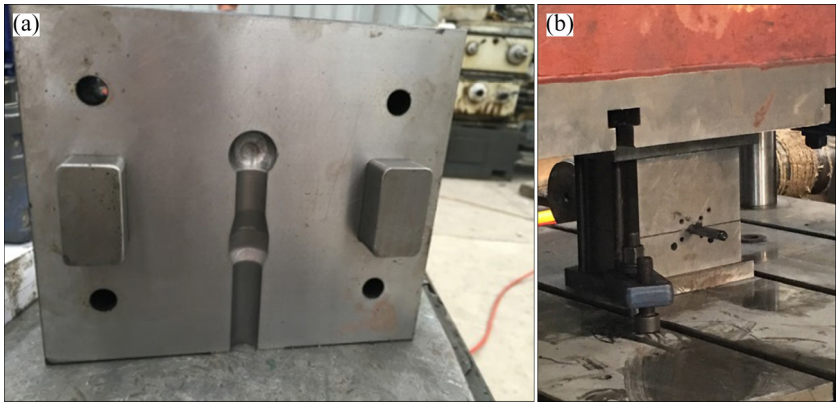

Fig. 3 Macrograph of half ECAEE-SC bottom die (a) and die sets employed for conducting ECAEE-SC experiments (b)

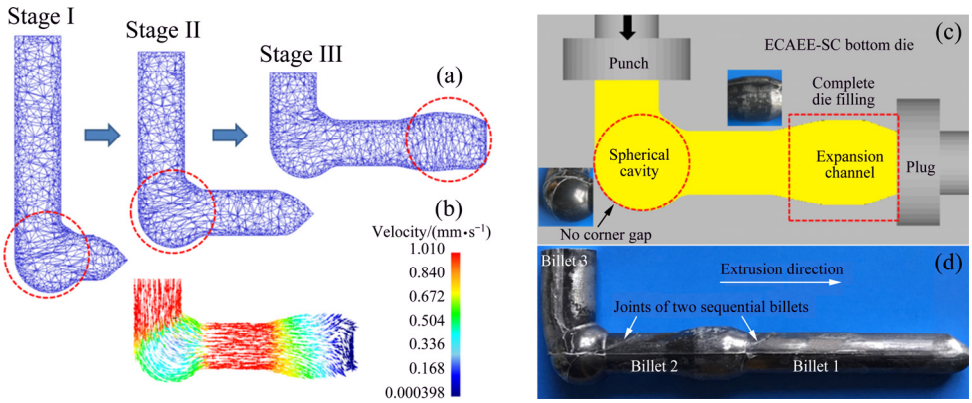

Fig. 4 Material flow of commercially pure aluminum billet during ECAEE-SC process: (a) Deformation of finite element mesh; (b) Velocity field recorded by FEM; (c) Rather complete die filling; (d) Appearance of ECAEE-SC processed billets

during the process, the ends of two sequential billets are jointed together as indicated by arrows in Fig. 4(d), and the appearance of ECAEE-SC processed billet by FEM simulation is consistent with that of the experiment (by comparing Fig. 4(d) with Fig. 4(a)).

Figure 5 represents the variation of the load versus the punch displacement obtained from FEM simulation corresponding to ECAEE-SC process, and the load−punch displacement curve for conventional ECAE process is provided for comparison. It is clear that the load history during ECAEE-SC process depends on the die design and can be interpreted into three stages. (1) Stage I: In the initial stage, the billet is compressed by the punch and continuously fills the spherical cavity with increased diameter. Since various deformation forms including shear, expansion and extrusion are generated simultaneously in the spherical corner, larger plastic strains are accumulated and accordingly, the load dramatically increases as compared with the conventional ECAE process. (2) Stage II: After the spherical cavity fully fills with the material, the head of processed billet enters into the horizontal transition channel and returns to its initial shape, and the process reaches a steady-state condition. Therefore, the load value maintains almost constant. (3) Stage III: As the process continues, the billet moves forward along the extrusion direction and then is extruded into the expansion channel where the additional simple shear strain is imposed on the material [19]. Accordingly, the load increases again with an intensive rate until the end of the process and finally reaches the peak value of about 94.5 kN, which is much higher than that of ECAE. Afterwards, the billet is extruded into the exit channel while no change in the cross-section happens. At this situation, the plug is removed and the extruded billet then acts as a plug, ensuring the expansion channel to remain fully filled during the process. Finally, as the final exit channel is precisely similar to the entry channel, the extruded billet experiences no deformation and finds the way out of the die.

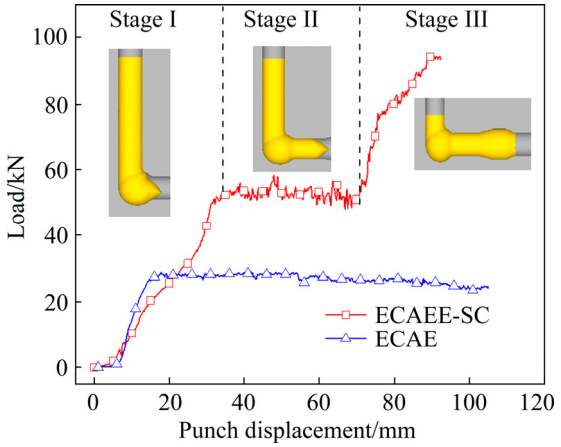

Fig. 5 Load−punch displacement curves obtained by FEM simulations under ECAEE-SC and ECAE processes

In addition, it should be mentioned that as the deformation of billet is constrained in a closed die cavity, the reduction of the channel diameter of exit channel and friction result in a high opposite force against the movement of the billet during deformation, which acts similarly to the back

pressure and forces the billet to achieve more pronounced filling in the die channel [20]. Therefore, the material plasticity and deformation homogeneity are greatly improved. Generally, the newly developed ECAEE-SC process is capable of "single-pass extrusion and multiple deformations", which can be regarded as a continuous process and is very promising for improving the efficiency of SPD process.

4.2 Effective plastic strain distribution

Figure 6 shows the effective strain contours in longitudinal section of the billet during ECAEE-SC process. As it indicates, ECAEE-SC process provides the possibility to accumulate larger plastic strain during a single pass. It can be seen that by the continuation of ECAEE-SC process, the effective strain imposed on the billet increases and the strain distribution becomes more and more homogeneous. This improvement is most likely related to the friction and back pressure created during the process. Due to a rather complete die filling of the processed billet, the material plasticity is significantly improved, which allows easy movement of the material throughout the die channels. So, the processed billet could endure larger deformation with an acceptable homogeneity [21]. According to Fig. 6(d), after a single pass of ECAEE-SC process, a large and steady deformation zone is formed within the processed billet except for a small part in the head and tail, and an average strain of 3.46−3.65 is stored in the billet.

In order to further quantitatively investigate the plastic strain distribution of commercially pure aluminum billet during ECAEE-SC process, nine tracking points in the steady deformation zones on both central and longitudinal cross-sections of the processed billet are selected respectively, and the variations of effective strain values are illustrated in Fig. 7. As is clearly visible in Fig. 7, both strain variation profiles are almost stable with minor fluctuations, denoting that the strain distribution within the billet is homogeneous. It should also be noticed that the strain gradually decreases from the periphery to the center, which may be attributed to the friction between the billet and die walls. As the billet surfaces are in contact with the die walls and thus subjected to the additional shear deformation which is caused by friction, the effective strain accumulated in these areas is larger than that of the central area. As Fig. 7 demonstrates, a single pass of ECAEE-SC is capable of imposing an average effective strain of about 3.51 on the material, which is over twice larger than that of the conventional ECAE process according to the

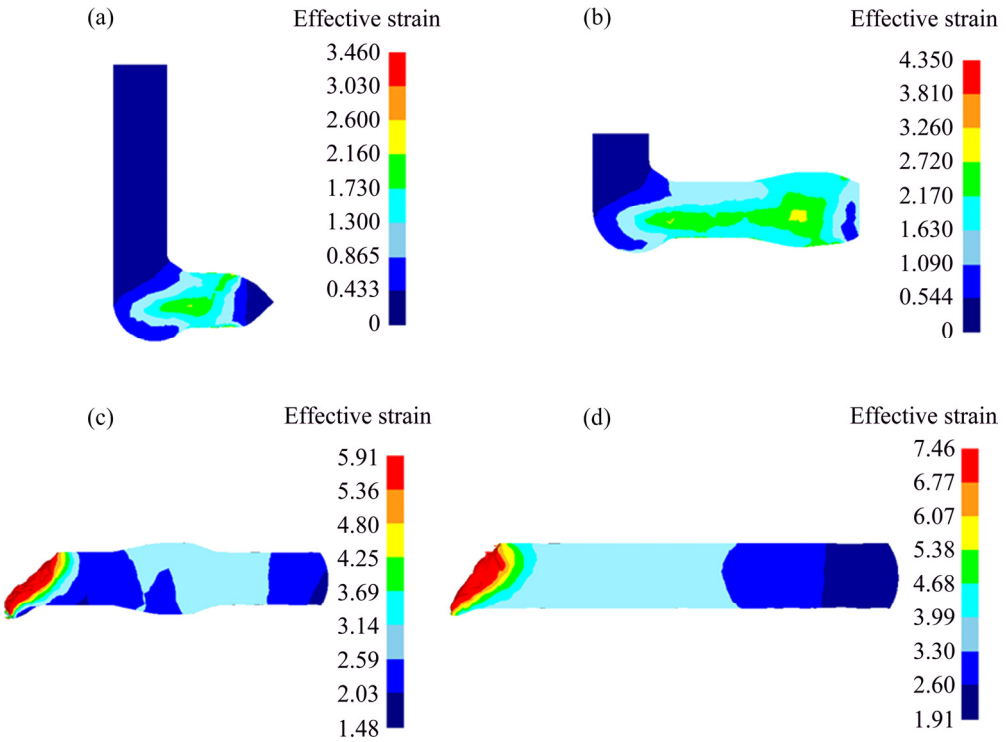

Fig. 6 Effective strain distribution in longitudinal direction of ECAEE-SC processed billet: (a) Initial deformation stage; (b) Stable deformation stage; (c) Expansion extrusion stage; (d) After single pass extrusion

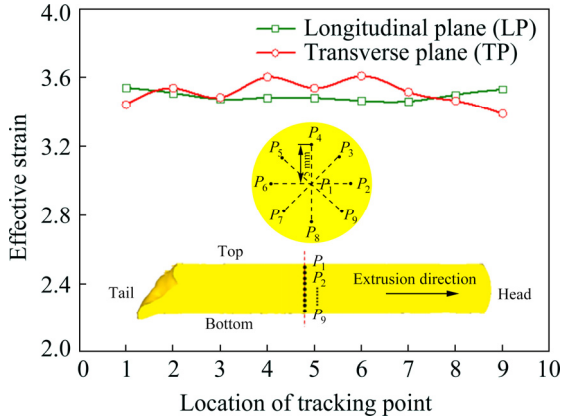

Fig. 7 Effective plastic strain distributions of ECAEE-SC processed billet

theoretical calculation based on the geometrical parameters of the fabricated die (~1.05) proposed by IWAHASHI et al [22]. Thus, it is believed that ECAEE-SC process can be used as a novel SPD method for plastic strain accumulation, which can lead to higher levels of plastic strain as well as more homogeneous distribution within the billet.

4.3 Mean stress distribution

Figure 8 depicts the evolution of mean stress distribution on the central longitudinal cross-section of the billet predicted by FEM during ECAEE-SC process. As seen in Fig. 8, it is clear that due to the novel design of ECAEE-SC die, the hydrostatic pressure in the as-processed material increases gradually as the process continues. At the beginning of the operation, under the high pressure of punch, the billet is approximately upset and locally deformed at the intersection of channels, resulting in the extensive hydrostatic stress within the billet at this moment (Fig. 8(a)). Having passed through the spherical cavity, the hydrostatic pressure increases and leads to a rather complete die filling, as shown in Fig. 8(b). With the continuation of deformation, the billet moves forward with the close contact with the die walls due to the intrinsic back-pressure provided at the exit channel of the die. Therefore, the billet endures a high hydrostatic pressure, as shown in Fig. 8(c), which is beneficial to the welding of internal cracks in the materials. However, it should be noted that in the last stage of deformation, as the processed billet in the expansion channel is severely deformed and accumulates extremely high plastic strains, tensile stress state even appears in the surface area of some parts of the billet (Fig. 8(c)), which maybe leads to the opening of microcracks and mainly accounts for the failure of as-processed billet in actual ECAEE-SC experiment [23].

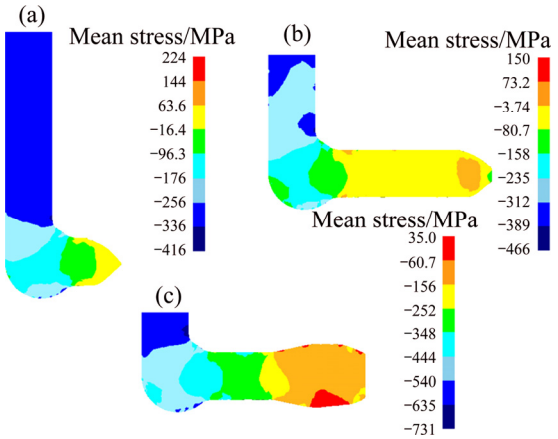

Fig. 8 Evolution of mean stress within billet at various stages during ECAEE-SC process: (a) At spherical cavity; (b) In transition channel; (c) In expansion channel

4.4 Microstructure characteristics

The orientation imaging analysis of commercially pure aluminum was performed in the middle of sample cross-section for the as-cast and the SPD-processed billets, respectively. The corresponding EBSD maps are illustrated in Fig. 9. As seen in Fig. 9(a), the microstructure of initial well-annealed aluminum consists of a large number of coarse equiaxed grains with the average diameter of more than 400 μm. It is clearly observed that single-pass ECAEE-SC exhibits higher efficiency of grain refinement and leads to more significant changes in the microstructure than conventional ECAE process (by comparing Fig. 9(b) with Fig. 9(c)). Due to the progressive strain accumulation imposed during ECAEE-SC process, the initial grains are elongated along the shear direction and severely broken into small band-like (or lamellar) or equiaxied grains, causing a notable decrease in the average grain size.

Figure 10 shows the grain size and grain boundary misorientation distributions of the processed pure aluminum after single-pass ECAEE-SC. As demonstrated in Fig. 10(b), although a very few of coarse grains can be seen in the microstructure, it is evident that almost 80% of grains are less than 20 μm in size after undergoing ECAEE-SC process (Fig. 10(a)). However, although the fractions of high angle grain

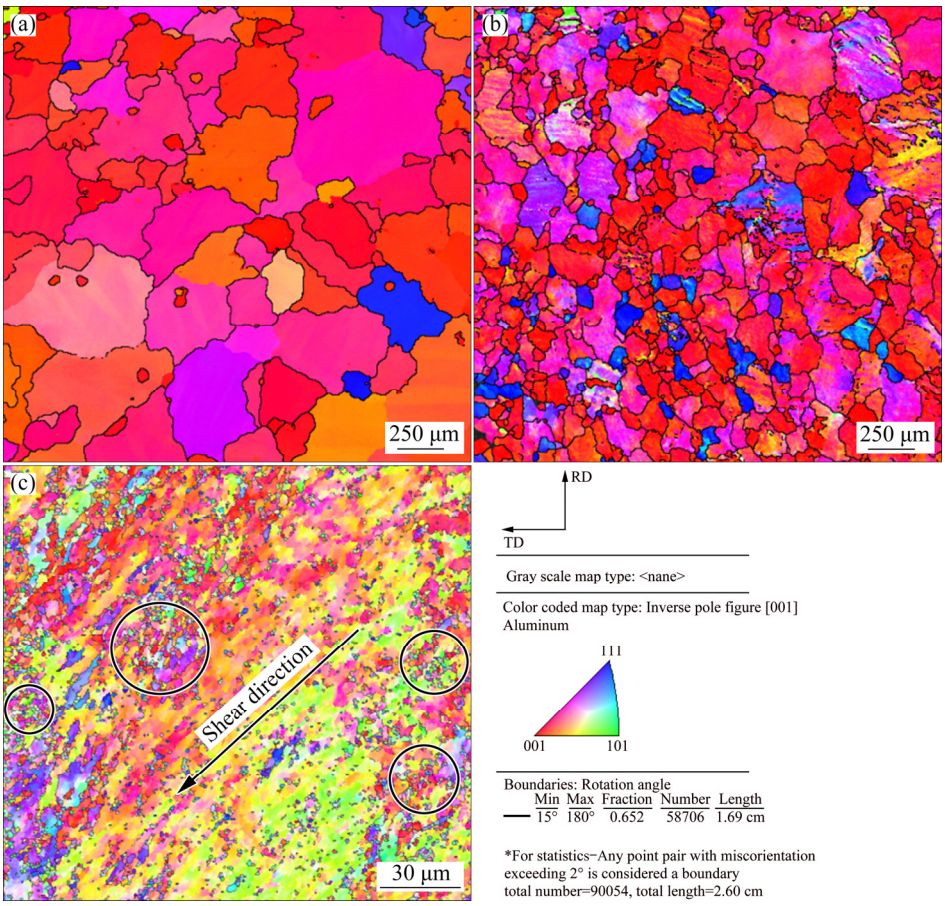

Fig. 9 Orientation maps of commercially pure aluminum billet: (a) As-received; (b) Single-pass ECAE; (c) Single-pass ECAEE-SC

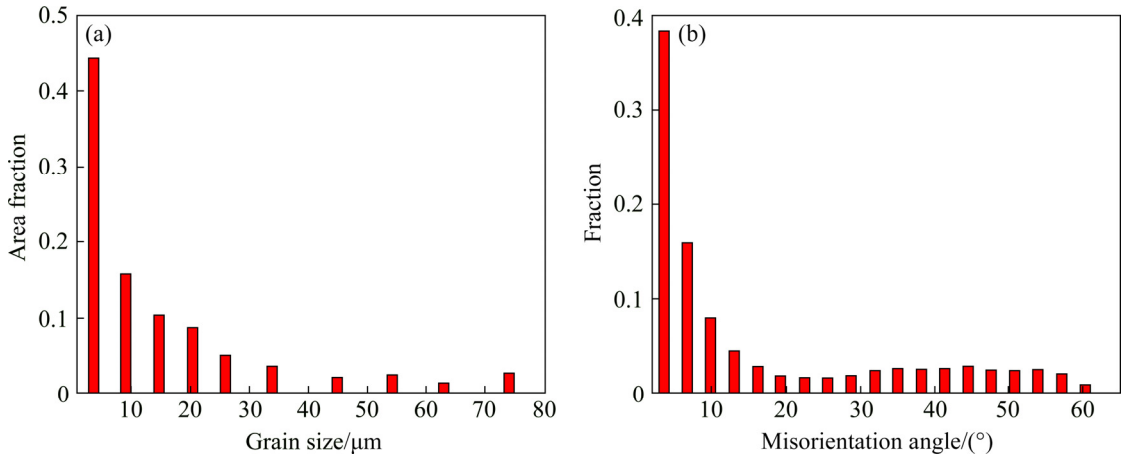

Fig. 10 Grain size (a) and grain boundary misorientation (b) distributions in as-processed aluminum after single-pass ECAEE-SC (corresponding to EBSD map in Fig. 9(c))

boundaries (HAGBs: misorientation >15°) are in the range of 36%−45% (Fig. 10(b)), many low angle grain boundaries (LAGBs) still exist in the microstructure, denoting that the microstructure exhibits new grains and highly developed subgrains. It is also worth noting that in some regions where the imposed plastic strain exceeds a critical value, dynamic recrystallization may occur as the nucleation of several new fine grains with HAGBs appears close to the banded grain boundaries (see circles in Fig. 9(c)). This may be correlated to the high hydrostatic pressure and large

plastic strain generated in the as-processed aluminum. Due to serious lattice distortion, extremely high density dislocations and distortion energy exist in the grain and subgrain boundaries, which lowers the activation energy for recrystallization start [24,25], and thus dynamic recrystallization can occur during ECAEE-SC process.

Further observations of the microstructure evolution were performed by TEM, as demonstrated in Fig. 11. It is found that in the early stage of ECAEE-SC process, a lot of parallel shear bands (Fig. 11(a)) with high density dislocations appear in the grains. With the increase of deformation, the entangled dislocations (Fig. 11(b)) gradually evolve into dislocation cells through rearrangement or elimination, forming subgrains with low angle grain boundaries (Fig. 11(c)). Afterwards, under the severe shear deformation or by grain rotation, large elongated areas are broken into small elongated or equiaxed subgrains, and eventually developed into equiaxed ultra-fine grains with high angle grain boundaries [26]. It is clearly seen in Fig. 11(d) that the UFG microstructure with sub-micron size less than 400 nm is obtained by conducting single-pass ECAEE-SC. Consequently, it is believed that in the present study, the grain refinement process mainly includes the generation of shear bands, the formation of cellular substructures, the appearance of subgrains with low angle grain boundaries and the formation of equiaxed ultrafine grains with high angle grain boundaries. The deformation mechanism of commercially pure aluminum during ECAEE-SC process at room temperature is dominated by dislocation slip with incomplete continuous dynamic recrystallization.

4.5 Microhardness evolution

Figure 12 represents the microhardness distribution on the central cross-section of as-processed aluminum billet under various conditions.

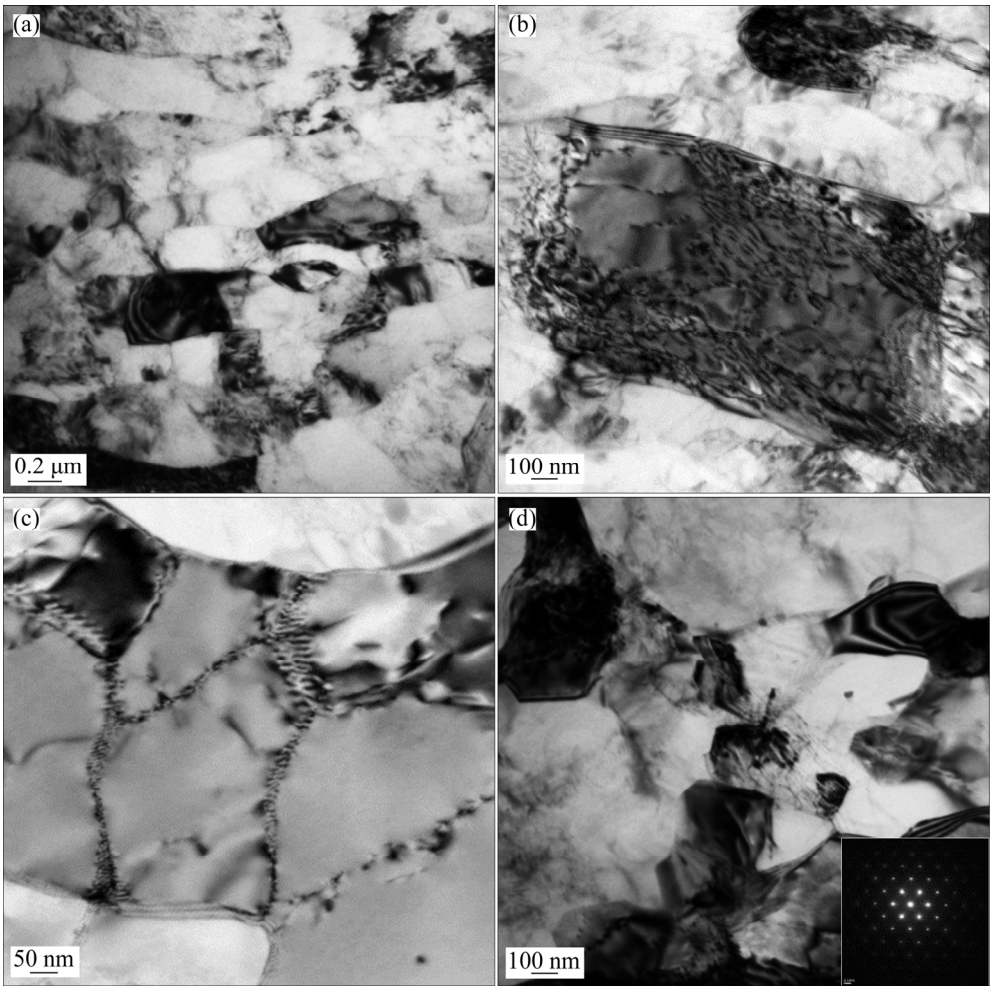

Fig. 11 TEM images and corresponding SAED patterns of UFG aluminum processed by ECAEE-SC: (a) Elongated shear bands; (b) Dislocation tangles in grains; (c) Formation of subgrains; (d) Grains with equiaxed microstructures

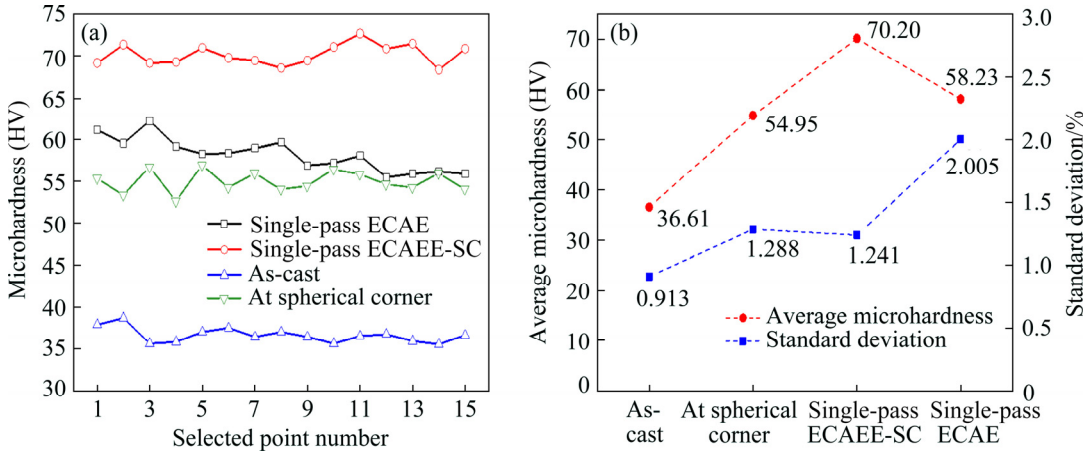

Fig. 12 Microhardness distribution (a), average microhardness and standard deviation (b) on central cross-sections of processed commercially pure aluminum billets

In order to better illustrate the strengthening effect of ECAEE-SC process, the results of microhardness measurement after single-pass ECAE were provided for comparison.

As Fig. 12 displays, for the initial as-cast commercially pure aluminum, the average microhardness value was about HV 36.61 with relatively homogeneous distribution. It is evident that the microhardness is significantly increased after single-pass of ECAEE-SC, and the average value increased to HV 70.20, denoting 91.75% improvement compared to that of the as-cast billet. The strengthening may be attributed to the extremely high plastic strains accumulated in the material, causing accumulation of dislocations and significant grain refinement. Based on the Hall−Petch relation, the reduction in the grain size could account for increasing the strength characteristics of the material [27]. Moreover, it can also be found that there is a large increase of the microhardness value from HV 36.61 to HV 54.95 when the billet undergoes severe plastic deformation at the spherical corner (see Fig. 12(a)), denoting the important role of this region in the enhancement of mechanical properties. Due to the "split-flow" of spherical cavity, the metal material at the corner is completely filled, and then continuously flows to the horizontal channel. The coupling effect of "expansion−shear−extrusion" in this region makes greater amount of plastic strain accumulated in the material, resulting in high dislocation density and exceptional grain refinement. In the subsequent expansion extrusion, the intrinsic back-pressure to the exit channel of the die is introduced to obtain larger deformation in the material, and to prevent defect formation on the surface of the billet during ECAEE-SC process. Therefore, the microhardness was further increased to HV 70.20 with more homogeneous distribution when compared to that of conventional single-pass ECAE process. In addition, it is clearly seen that the evolution of microhardness correlates well with the strain distribution mentioned above, which is in acceptance with the results of previous numerical simulation.

5 Conclusions

(1) ECAEE-SC process has a high efficiency for material forming by integrating various successive deformations including upsetting, expansion, shear and extrusion in single pass. During ECAEE-SC process, the spherical corner and the expansion channel are two main deformation zones. The load variations can be interpreted into three stages showing a tendency of "sharp increase, relatively steady and further increase".

(2) ECAEE-SC process can be used as a novel and effective SPD method for strain accumulation. During the process, the material is under an ideal hydrostatic stress state, which can notably prevent the microcracks of the processed billet and improve its workability. After one pass of ECAEE-SC, the accumulated effective strain is up to 3.51 and the homogeneity of strain distribution is considerably improved within the billet, exhibiting higher deformation efficiency compared with the

conventional ECAE process.

(3) Due to the intense plastic strain as well as large hydrostatic pressure applied during the process, the grains of commercially pure aluminum billet were significantly refined after single-pass of ECAEE-SC. The microstructure consists of many highly developed subgrains, and the nucleation of equiaxed ultrafine grains with sub-micro grain size less than 400 nm occurs instead, indicating that the deformation mechanism of commercially pure aluminum during ECAEE-SC process at room temperature is dominated by dislocation slip with incomplete continuous dynamic recrystallization.

(4) The microhardness of ECAEE-SC processed billet was increased from HV 36.61 to HV 70.20, showing 91.75% enhancement compared with that of the as-cast billet. Moreover, the homogeneity of microhardness distribution is considerably improved, which correlates well with the strain distribution obtained from FEM and verifies the numerical simulation results.

References

[1] LANGDON T G. Twenty-five years of ultrafine-grained materials: Achieving exceptional properties through grain refinement [J]. Acta Materialia, 2013, 61(19): 7035−7059.

[2] HARSHA R N, MITHUN KULKARNI V, SATISH BABU B. Severe plastic deformation—A review [J]. Materials Today: Proceedings, 2018, 5(10): 22340−22349.

[3] LANGDON T G. Processing of ultrafine-grained materials using severe plastic deformation: Potential for achieving exceptional properties [J]. Revista de Metalurgia, 2008, 44(6): 556−564.

[4] WANG Cheng-peng, LI Fu-guo, CHEN Bo, YUAN Zhan-wei, LU Hong-ya. Severe plastic deformation techniques for bulk ultrafine-grained materials [J]. Rare Metal Materials and Engineering, 2012, 41(6): 941−946.

[5] VALIEV R, LANGDON T G. Principles of equal-channel angular pressing as a processing tool for grain refinement [J]. Progress in Materials Science, 2006, 51(7): 881−981.

[6] FRINT P, WAGNER M F X. Strain partitioning by recurrent shear localization during equal-channel angular pressing of an AA6060 aluminum alloy [J]. Acta Materialia, 2019, 176: 306−317.

[7] TOTH L S, GU C F. Ultrafine-grain metals by severe plastic deformation [J]. Materials Characterization, 2014, 92: 1−14.

[8] IVANISENKO YU, KULAGIN R, FEDOROV V, MAZILKIN A, SCHERER T, BARETZKY B, HAHN H. High pressure torsion extrusion as a new severe plastic deformation process [J]. Materials Science and Engineering A, 2016, 664: 247−256.

[9] DJAVANROODI F, EBRAHIMI M. Effect of die parameters and material properties in ECAP with parallel channels [J]. Materials Science and Engineering A, 2010, 527: 7593−7599.

[10] SHIMA S, TORBATI S, SEYED A, LANGDON T G. An investigation of the limits of grain refinement after processing by a combination of severe plastic deformation techniques: A comparison of Al and Mg alloys [J]. Materials Science and Engineering A, 2018, 712: 373−379.

[11] WANG Xiao-xi, HE Min, ZHU Zhen, XUE Ke-min, LI Ping. Influence of twist extrusion process on consolidation of pure aluminum powder in tubes by equal channel angular pressing and torsion [J]. Transactions of Nonferrous Metals Society of China, 2015, 25: 2122−2129.

[12] FADAEI A, FARAHAFSHAN F, SEPAHI-BOROUJENI S. Spiral equal channel angular extrusion (Sp-ECAE) as a modified ECAE process [J]. Materials & Design, 2017, 113: 361−368.

[13] FERESHTEH-SANIEE F, ASGARI M, BARATI M, PEZESHKI S M. Effects of die geometry on non-equal channel lateral extrusion (NECLE) of AZ80 magnesium alloy [J]. Transactions of Nonferrous Metals Society of China, 2014, 24: 3274−3284.

[14] MUHAMMAD J Q, GIRIBASKAR S, ANDRZEJ R. Effect of incremental equal channel angular pressing (I-ECAP) on the microstructural characteristics and mechanical behavior of commercially pure titanium [J]. Materials & Design, 2017, 122: 385−402.

[15] KIM K, YOON J. Evolution of the microstructure and mechanical properties of AZ61 alloy processed by half channel angular extrusion (HCAE): A novel severe plastic deformation process [J]. Materials Science and Engineering A, 2013, 578: 160−166.

[16] SEPAHI-BOROUJENI S, FERESHTEH-SANIEE F. The influences of the expansion equal channel angular extrusion operation on the strength and ductility of AZ80 magnesium alloy [J]. Materials Science and Engineering A, 2015, 636: 249−253.

[17] Scientific Forming Technologies Corporation. DEFORM TM 3D Version 6.1: User's manual scientific forming technologies corporation [M]. Columbus, Ohio: Scientific Forming Technologies Corporation, 2004.

[18] MOHAMED IBRAHIM A EL AAL. 3D FEM simulations and experimental validation of plastic deformation of pure aluminum deformed by ECAP and combination of ECAP and direct extrusion [J]. Transactions of Nonferrous Metals Society of China, 2017, 27: 1338−1352.

[19] WANG Cheng-peng, LI Fu-guo, LI Qing-hua, WANG Lei. Numerical and experimental studies of pure copper processed by a new severe plastic deformation method [J]. Materials Science and Engineering A, 2012, 548: 19−26.

[20] ALAVIZADEH S M, ABRINIA K, PARVIZI A. Twisted multi-channel angular pressing (TMCAP) as a novel severe plastic deformation method [J]. Metals and Materials International, 2020, 26: 260−271.

[21] RAHIMI F, EIVANI A R, KIANI M. Effect of die design parameters on the deformation behavior in pure shear extrusion [J]. Materials & Design, 2015, 83: 144−153.

[22] IWAHASHI Y, YANG J, HORITA Z, NEMOTO M, LANGDON T G. Principle of equal-channel angular pressing for the processing of ultra-fine grained materials [J]. Scripta

Materilia, 1996, 52(2): 143−146.
[23] YOON S C, JEONG H G, LEE S, KIM H S. Analysis of plastic deformation behavior during back pressure equal channel angular pressing by the finite element method [J]. Computational Materials Science, 2013, 77: 202−207.
[24] KOIZUMI T, KURODA M. Grain size effects in aluminum processed by severe plastic deformation [J]. Materials Science and Engineering A, 2018, 710: 300−308.
[25] TOLAMINEJAD B, HOSEINI-ATHAR M M. An investigation of microstructure and mechanical properties during ECAE of commercially pure aluminum [J]. Materials Science and Engineering A, 2016, 670: 146−152.
[26] NAJAFI S, EIVANI A R, SAMAEE M, JAFARIAN H R, ZHOU J. A comprehensive investigation of the strengthening effects of dislocations, texture and low and high angle grain boundaries in ultrafine grained AA6063 aluminum alloy [J]. Materials Characterization, 2018, 136: 60−68.
[27] HU Hong-jun, LIU Yang, ZHANG Ding-fei, OU Zhong-wen. The influences of extrusion-shear process on microstructures evolution and mechanical properties of AZ31 magnesium alloy [J]. Journal of Alloys and Compounds, 2017, 695: 1088−1095.

等通道球形转角膨胀挤压工业纯铝的剧烈塑性变形行为

王晓溪[1]， 张 翔[2,3]，井新宇[1]，袁峻池[1]，宋 威[1]

1. 徐州工程学院 机电工程学院，徐州 221018；
2. 江苏徐工工程机械研究院有限公司，徐州 221004；
3. 徐工集团 高端工程机械智能制造国家重点实验室，徐州 221004

摘 要：提出一种耦合强塑性应变与高静水压力于一体的新型剧烈塑性变形工艺——等通道球形转角膨胀挤压(ECAEE-SC)。采用三维有限元数值模拟分析软件 DEFORM-3D 研究工业纯铝在 ECAEE-SC 变形过程中的塑性变形行为，分析材料流动、挤压载荷、等效应变和平均应力的分布规律，并与传统 ECAE 工艺进行比较。开展工业纯铝室温单道次 ECAEE-SC 变形验证实验，探讨材料显微组织和显微硬度的演变规律。结果表明，在 ECAEE-SC 变形过程中，材料内部处于理想的静水压力状态，挤压变形所需载荷较传统 ECAE 工艺时大幅增加。经单道次变形后，坯料内部累积塑性应变量达 3.51 且变形均匀性良好；工业纯铝晶粒得到显著细化，内部形成亚微米级等轴超细晶组织；材料显微硬度均匀分布，硬度值由初始铸态的 HV 36.61 提高到 HV 70.20，增幅达 91.75%。

关键词：剧烈塑性变形；等通道球形转角膨胀挤压；数值模拟；应变累积；晶粒细化

(Edited by Wei-ping CHEN)